Acta Crystallographica Section D
Biological Crystallography
ISSN 0907-4449

Interactions of *Streptomyces griseus* aminopeptidase with a methionine product analogue: a structural study at 1.53 Å resolution

R. Gilboa,[a] H. M. Greenblatt,[a] M. Perach,[b] A. Spungin-Bialik,[b] U. Lessel,[c] G. Wohlfahrt,[c] D. Schomburg,[c] S. Blumberg[b] and G. Shoham[a]*

[a]Department of Inorganic Chemistry and the Laboratory for Structural Chemistry and Biology, The Hebrew University of Jerusalem, Jerusalem 91904, Israel, [b]Sackler Institute of Molecular Medicine, Department of Human Genetics and Molecular Medicine, Sackler Faculty of Medicine, Tel Aviv University, Tel Aviv 69978, Israel, and [c]Institute of Biochemistry, University of Cologne, Cologne 50674, Germany

Correspondence e-mail: gil2@vms.huji.ac.il

Received 17 November 1999
Accepted 9 February 2000

PDB References: SGAP, 1cp7; SGAP–Met, 1qq9.

SGAP is an aminopeptidase present in the extracellular fluid of *Streptomyces griseus* cultures. It is a double-zinc enzyme with a strong preference for large hydrophobic amino-terminus residues. It is a monomeric (30 kDa) heat-stable enzyme, with a high and efficient catalytic activity modulated by calcium ions. The small size, high activity and heat stability make SGAP a very attractive enzyme for various biotechnological applications. Only one other related aminopeptidase *(Aeromonas proteolytica* AP; AAP) has been structurally analyzed to date and its structure was shown to be considerably similar to SGAP, despite the low sequence homology between the two enzymes. The motivation for the detailed structural analysis of SGAP originated from a strong mechanistic interest in the family of double-zinc aminopeptidases, combined with the high potential applicability of these enzymes. The 1.75 Å crystallographic structure of native SGAP has been previously reported, but did not allow critical mechanistic interpretations owing to inconclusive structural regions around the active site. A more accurate structure of SGAP at 1.58 Å resolution is reported in this paper, along with the 1.53 Å resolution structure of the SGAP complex with inhibitory methionine, which is also a product of the SGAP catalytic process. These two high-resolution structures enable a better understanding of the SGAP binding mode of both substrates and products. These studies allowed the tracing of the previously disordered region of the enzyme (Glu196–Arg202) and the identification of some of the functional groups of the enzyme that are involved in enzyme–substrate interactions (Asp160, Met161, Gly201, Arg202 and Phe219). These studies also suggest that Glu131 is directly involved in the catalytic mechanism of SGAP, probably as the hydrolytic nucleophile. The structural results are compared with a recent structure of AAP with an hydroxamate inhibitor in order to draw general functional conclusions which are relevant for this family of low molecular-weight aminopeptidases.

1. Introduction

S. griseus aminopeptidase (SGAP) is one of the enzymes present in the extracellular fluid of *S. griseus* cultures. It is a double-zinc proteolytic enzyme with a strong preference for large hydrophobic amino-terminus residues. It is a monomer of relatively low molecular weight (30 kDa), is heat stable, displays a high and efficient catalytic turnover and its activity is modulated by calcium ions (Spungin & Blumberg, 1989; Ben-Meir *et al.*, 1993). The small size, high activity and heat stability make SGAP a very attractive enzyme for various

biotechnological applications, including the processing of recombinant DNA proteins and fusion-protein products (Ben-Bassat *et al.*, 1987; Nagakawa *et al.*, 1987; Ben-Meir & Blumberg, 1991). These properties also make SGAP an ideal tool for use in two-stage assays of other peptidases in diagnostic applications (Indig *et al.*, 1989, 1990).

The amino-acid sequence (Maras *et al.*, 1996) and the three-dimensional structure (Greenblatt *et al.*, 1997) of SGAP have recently been determined. Only one other low molecular-weight double-zinc aminopeptidase (*A. proteolytica* AP; AAP) has been structurally analyzed to date (Chevrier *et al.*, 1994). In spite of a sequence homology of only 30% (Maras *et al.*, 1996), SGAP and AAP show a structural similarity of about 70%, as measured by the method developed by Lessel & Schomburg (1994). The main differences in the topology of AAP and SGAP are an extra helix in AAP at the N-terminus and an extra helix in SGAP near the C-terminus. However, the two enzymes resemble each other very closely in their double-zinc coordination and are hence likely to have a common catalytic mechanism.

A related high molecular-weight enzyme, leucine aminopeptidase (LAP; Burley *et al.*, 1990, 1992), was shown to be significantly different in both structure and sequence. LAP is a hexamer in which each monomer is built of two structural domains. One of these domains, the catalytic domain containing the double-zinc active site, has a relatively similar overall topology to SGAP and AAP, but contains several additional secondary-structural units. Despite this relative similarity in overall structure, the active site of LAP differs significantly from those of SGAP and AAP, especially in the nature of the zinc ligands and the symmetry between the two active-site Zn atoms.

Another low molecular-weight aminopeptidase for which the three-dimensional structure has been determined is methionine aminopeptidase (MAP; Roderick & Matthews, 1993). MAP contains two closely positioned cobalt ions in the active site corresponding to the two zinc ions in LAP, AAP and SGAP. Nevertheless, MAP bears no resemblance to any of these enzymes at either the sequence or the structural level and hence is considered to represent a separate class of aminopeptidases.

SGAP crystals belong to the tetragonal space group $P4_12_12$, with unit-cell parameters $a = b = 61.82$, $c = 145.88$ Å and one molecule of SGAP in the asymmetric unit (Almog *et al.*, 1993). The 1.75 Å resolution crystal structure of SGAP (Greenblatt *et al.*, 1997) showed that the main core of the protein is constructed of an eight-stranded (parallel and antiparallel) β-sheet surrounded by α-helices on either side. The active site was located at the bottom of a small cleft on one side of the molecule created by the carbonyl ends of two of the central β-sheet strands. It was shown to contain two zinc cations, each coordinated to five ligands which are similar in both chemical nature and geometry, at a zinc–zinc distance of 3.6 Å. A heptacoordinated calcium-binding site has been located around the amino-terminus region of the protein at a distance of about 25 Å from the active-site zinc cations. The calcium ion seems to rigidify the amino-terminus region of the enzyme; however, its role in the overall catalytic activity of SGAP is not completely understood.

While the three-dimensional structure of SGAP is known at relatively high resolution, no structural information is available on any of its complexes with substrates, substrate analogues or inhibitors. As a result, very little is known about the mode of binding of the enzyme, the specific functional groups involved in catalysis and the various steps involved in the catalytic reaction. Moreover, two sections of the polypeptide chain could not be traced owing to poor electron density in the original 1.75 Å maps (Greenblatt *et al.*, 1997): one stretch of six residues (Glu196–Gly201) which borders the active site and the final seven C-terminal residues starting with Gly278. In addition, a presumed phosphate ion (probably abstracted from the crystallization solution) was found to be bound to the catalytic zinc ions of the original structure and made it difficult to evaluate the normal substrate binding in the SGAP active site. In order to resolve some of these important structural issues, we conducted a detailed structural study of a phosphate-free native SGAP as well as its complex with an inhibitory methionine. Here, we report the crystallographic structural analysis of native SGAP at 1.58 Å resolution, together with a complementary analysis of the SGAP–Met complex at 1.53 Å resolution. These structures provide a detailed three-dimensional architecture of the SGAP active site, point out some of the critically important amino-acid residues, suggest a general mode of substrate binding and enable the exploration of the catalytic mechanism of this enzyme by molecular modelling.

2. Materials and methods

Native SGAP was purified and crystallized as described previously (Spungin & Blumberg, 1989; Almog *et al.*, 1993; Greenblatt *et al.*, 1997). High-resolution diffraction data to 1.58 Å was measured on a single crystal of SGAP using a MAR Research (MAR300) imaging-plate area detector ($\lambda = 1.15$ Å) at the X26C beamline, NSLS synchrotron facility, Brookhaven National Laboratories (New York, USA). All imaging-plate raw diffraction data were processed with the *DENZO* and *SCALEPACK* software (Otwinowski, 1991) to give the final merged intensity data set. Representative measurement statistics for this data are shown in Table 1, where they are also compared with corresponding parameters from the old native SGAP data and the new SGAP–Met data.

The initial model used for electron-density calculations was the original SGAP structure at 1.75 Å resolution (Greenblatt *et al.*, 1997; PDB entry 1xjo); difference Fourier procedures were used to build missing segments. Two subsequent rounds of simulated annealing and five additional rounds of refinement with individual temperature factors (*CNS*; Brunger *et al.*, 1998) and model building (*O*; Jones *et al.*, 1991) yielded the final model. The structure was manually inspected with simulated-annealed omit maps and weighted $2F_o - F_c$ and $F_o - F_c$ electron-density maps; the refinement progress was confirmed by the steady decrease in both the R factor and $R_{\rm free}$. In the final cycles of refinement, these values converged

Table 1
Crystallographic data and refinement parameters for native SGAP and the SGAP–Met complex.

Native SGAP (1), old structure at 1.75 Å resolution; native SGAP (2), new structure at 1.58 Å resolution.

	Native SGAP (1)	Native SGAP (2)	SGAP–Met
Unit-cell parameters (Å)			
$a = b$	61.81	61.75	61.93
c	146.2	146.15	146.64
No. of unique reflections	28606	37354	42800
Resolution (Å)	20–1.75	32–1.58	32–1.53
Completeness (last shell) (%)	96.9	94.0 (63.2)	97.5 (69.8)
$\langle I/\sigma \rangle$	14.0	12.7	17.2
R_{sym}† (last shell) (%)	5.4	4.5 (14.1)	5.8 (20.3)
No. of protein atoms	1992	2032	2055
No. of solvent molecules	253	251	294
R factor (R_{free})‡ (%)	14.1	14.4 (17.1)	14.8 (17.3)
R.m.s. deviations from ideal geometry			
Bond lengths (Å)	0.02	0.019	0.019
Bond angles (°)	2.8	1.9	1.9

† $R_{sym} = (\sum|I - \langle I \rangle|)/\sum I$, excluding single measurements. ‡ R factor and $R_{free} = (\sum||F_o| - |F_c||)/\sum|F_o|$, for reflections in the working (R factor) and test (R_{free}) sets, respectively. For the test set, 10% of the total reflections (randomly picked) were used.

to an R factor of 14.4%, an R_{free} of 17.1% and excellent stereochemical parameters, as listed in Table 1.

Single crystals of the SGAP–Met complex were originally grown over a period of 3–4 months by the hanging-drop vapour-diffusion method. The protein solution contained 18 mg ml^{-1} SGAP in 10 m*M* Tris–HCl pH 8.0, 20 m*M* NaCl, 6 m*M* $CaCl_2$ and 100 m*M* methionine. The protein crystallization drops consisted of a mixture of equal volumes of the protein solution and a precipitant solution containing 24%(*w*/*v*) PEG 4000 and 0.1 *M* ammonium sulfate. These drops were equilibrated against a 1 ml reservoir of the precipitant solution. Microseeding techniques were later used in order to accelerate the crystallization process to 3–4 d. For the micro-seeding procedure, a well formed (small) crystal was taken and moved to a drop (60 µl) containing diluted precipitant solution. Once the crystal had been transferred, it was thoroughly crushed and the drop was thoroughly mixed. The freshly made solution containing the microcrystals was then transferred to the target protein/precipitant drops (equilibrated previously against 1 ml reservoir of the precipitant solution for about 24 h). In this case, the precipitant solution contained only 18% PEG 4000 (compared with 24% in the original procedure). Experiments indicated that crystals would not grow without seeding at this concentration of PEG. Under these conditions, crystals initially appeared within 3–4 d of seeding and grew to their full size (average dimensions of 0.8 × 0.3 × 0.2 mm) within a further week.

High-resolution data to 1.53 Å was measured on a single SGAP–Met crystal at room temperature using the X26C/NSLS experimental set-up described above for the native enzyme. Representative diffraction and refinement parameters are listed in Table 1. Since the SGAP–Met crystals were found to be completely isomorphous to the crystals of native SGAP ($P4_12_12$ space group and less than 2% difference in the unit-cell parameters), we used the 1.58 Å structure of native SGAP (described above) as the initial model. Difference Fourier calculations were used to locate the bound methionine residue, as well as to determine the conformational changes in the active site caused by the methionine binding. Structure refinement (*CNS*; Brunger *et al.*, 1998) and model building (*O*; Jones *et al.*, 1998) were then used to obtain the final structure (Table 1) as described above. The electron-density difference maps showed very clearly the bound methionine in the SGAP active site (Fig. 1), enabling a straightforward identification of all of its non-H atoms.

A pseudo-substrate was modelled with *BRAGI* (Schomburg & Reichelt, 1988) into the enzyme's active site by adding two alanine residues to the C-terminus of the bound methionine inhibitor in the SGAP–Met complex structure, in such a way that they approximately follow the open channel which is observed in the hydrophobic surface of the enzyme. The water, respectively the hydroxide ion, observed in the native SGAP structure at 1.58 Å resolution, was introduced as a potential nucleophile. Each modelled complex was energy-minimized, equilibrated by molecular dynamics for 100 ps at 298 K and analyzed for a further 100 ps. The *AMBER* 4.1 program package (Pearlman *et al.*, 1995) was used for the force-field calculations with an all-atom force field (Cornell *et al.*, 1995) and additional parameters for zinc (Hoops *et al.*, 1991). 12 crystallographic water molecules from the active-site region were added to the system and the space within a 12 Å radius of the active-site Zn1 was filled with water molecules. Only the atoms of the residues inside this 12 Å radius were allowed to move during the simulations.

3. Results and discussion

3.1. The structure of native SGAP at 1.58 Å resolution

The refined crystal structure of native SGAP consists of 275 of the 284 residues of the protein and 251 solvent water

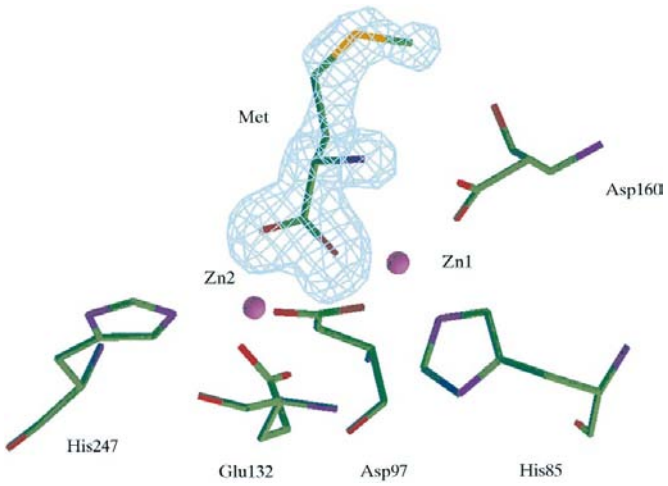

Figure 1
Electron-density difference (omit) map ($F_o - F_c$ coefficients) for the final structure of the SGAP–Met complex, showing the observed density (contour level of 4σ, cyan) for the bound methionine (Met) in the active site of the enzyme.

molecules. In this structure, we were able to identify a single water molecule which is bound to the two catalytic zinc ions and we were able to locate in the electron density three additional amino-acid residues (Glu196, Thr197, Glu198) in the missing active-site loop (Fig. 2, blue model). The thermal parameters of these residues (average value of 41.8 Å^2, compared with 16.8 Å^2 in other regions of the protein) and the lack of electron density for the three adjacent residues (199–201) suggest that this loop is considerably flexible in the native enzyme. However, the newly built partial structure of this loop indicates that it forms a critical part of a deep and narrow substrate-binding pocket. It also suggests that the observed flexibility of this loop may be needed to enable the entrance of an incoming substrate into the deep pocket. This particular loop seems to be much less flexible when a substrate (or inhibitor) is bound to the active site (Fig. 2, red model), as demonstrated in the SGAP–Met structure below.

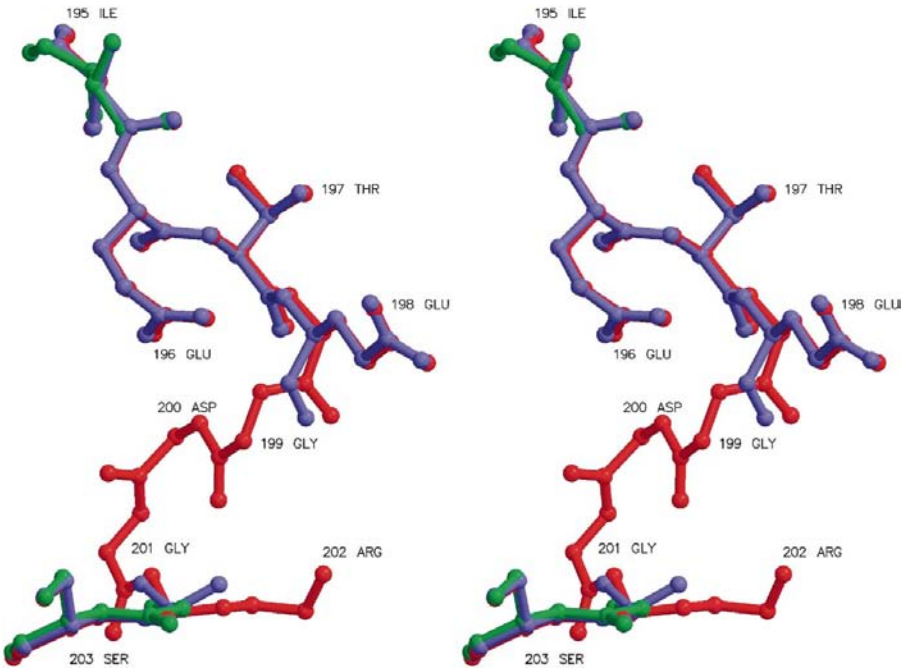

Figure 2
A stereoview superposition of the 'flexible loop' region of SGAP as determined for the native enzyme at 1.75 Å resolution (green), the native enzyme at 1.58 Å resolution (blue) and the SGAP–Met complex at 1.53 Å resolution (red).

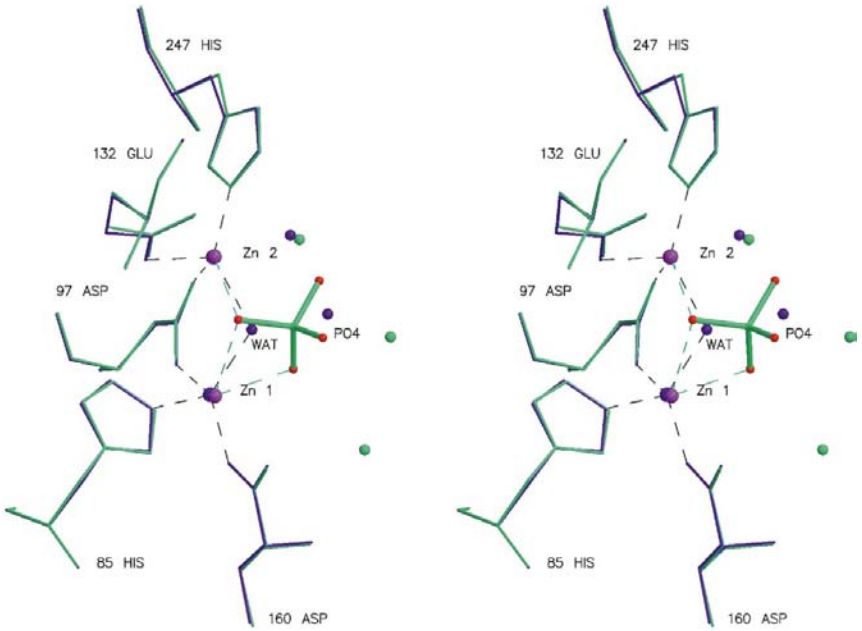

Figure 3
Stereoview of the SGAP active site. The refined new structure of the native enzyme at 1.58 Å (blue) is superimposed on the old structure of the native enzyme at 1.75 Å (green). It is demonstrated that most of the active site is identical, except for the non-protein ligand of the active-site zinc ions [a phosphate ion (PO4) for the old structure and a water molecule (WAT) for the new structure] observed approximately in the same coordination site between the two metal ions (Zn1 and Zn2). The difference in this zinc ligand is probably the main factor causing positional differences for the active-site water molecules between the old (green) and the new (blue) structures.

As in the previously reported structure, in the newly refined structure the active site of SGAP contains two zinc ions, at a Zn–Zn distance of 3.6 Å. Each of the zinc ions has one imidazole group (His85 for Zn1 and His247 for Zn2) and one carboxylate group (Asp160 for Zn1 and Glu132 for Zn2) as ligands. There is also an additional carboxylate group (Asp97) bridging the two zinc ions. The zinc-bound phosphate ion observed in the 1.75 Å structure of SGAP is not present in the current 1.58 Å native structure, probably as a consequence of materials (PEG, buffer *etc*.) of higher purity being used in the crystallization solutions. In turn, we located very clearly a bridging water molecule (or a hydroxide ion) in the exact position previously occupied by one of the phosphate O atoms (Fig. 3). The O atom of this bridging ligand is bound almost symmetrically to both zinc ions (2.16 Å to Zn1 and 2.28 Å to Zn2). Each of the active-site zinc ions in SGAP is hence coordinated to three protein ligands and a water/hydroxide ligand in a distorted tetrahedral geometry.

A similar double-zinc coordination has been reported for the structurally homologous AAP (Chevrier *et al.*, 1994), including the three protein ligands to each zinc ion and the bridging water/hydroxide ligand (Fig. 4). The

Zn—O distances for this bridging ligand are 2.25 and 2.29 Å for Zn1 and Zn2, respectively (note that the assignment of Zn1 and Zn2 is reversed in AAP compared with SGAP). The similarity of the fourth (bridging) ligand is especially interesting, since it is thought that this 'labile' coordination site is universally used for substrate binding and activation for hydrolysis, as demonstrated by the structure of the AAP complex with an hydroxamate analogue (Chevrier *et al.*, 1996) and the structure of LAP with L-leucinal (Strater & Lipscomb, 1995).

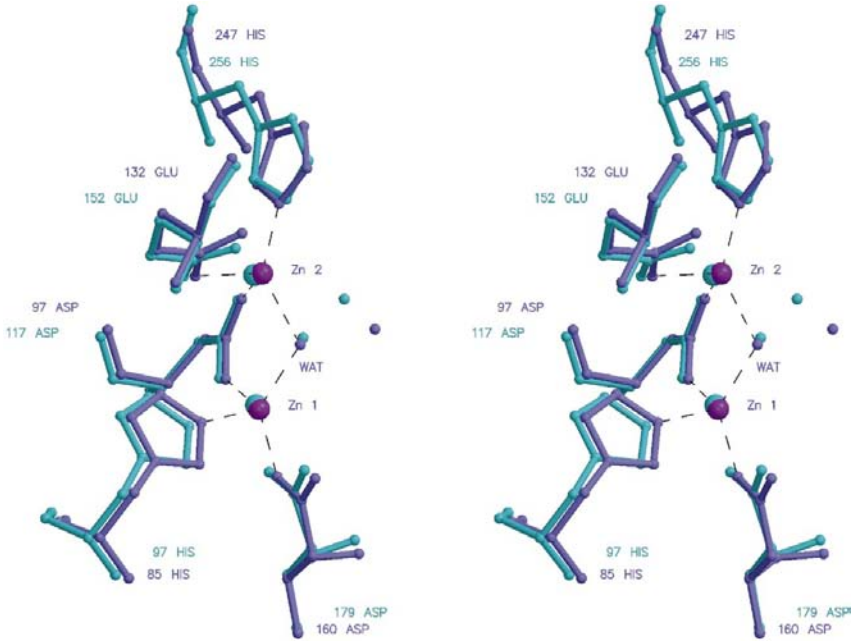

Figure 4
Stereoview comparison of the active site of SGAP (1.58 Å structure, blue) and the active site of AAP (1.8 Å structure, cyan), demonstrating a high degree of structural similarity in the zinc environment despite the low degree of overall sequence homology. The Zn atoms of the SGAP structure are shown in purple.

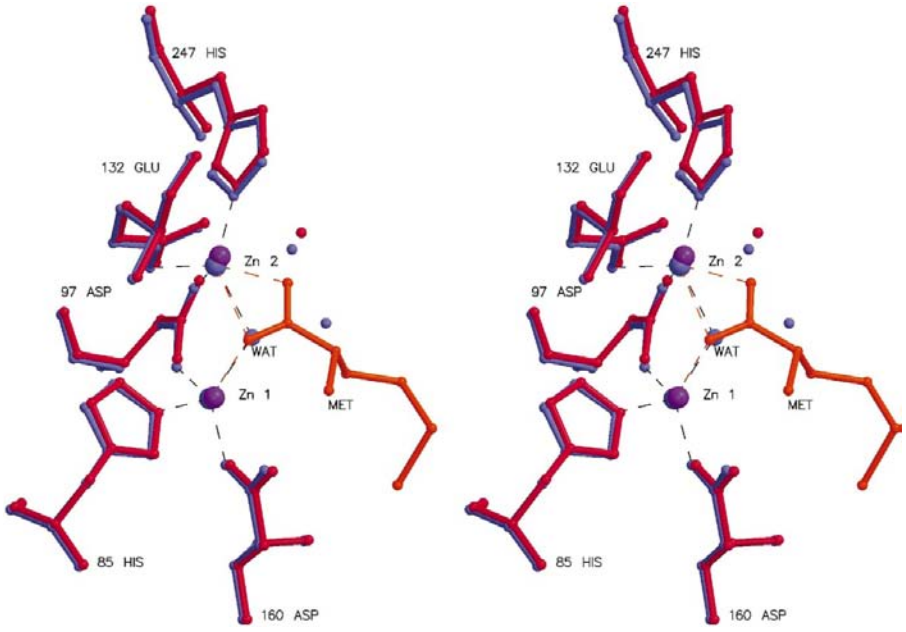

Figure 5
Structural superposition of the zinc environments in native SGAP (1.58 Å resolution, blue) and the SGAP–Met complex (1.53 Å resolution, red). The active-site zinc ions of the SGAP–Met structure are shown in purple (Zn1 and Zn2) and the bound methionine (MET) in the SGAP–Met structure is shown in orange.

3.2. The structure of the SGAP–Met complex at 1.53 Å resolution

Our initial attempts to obtain structural information on the enzyme with bound analogues focused on inhibitory amino acids. Several free amino acids, such as phenylalanine, leucine and methionine (Met), act as medium-strength inhibitors of SGAP (K_i values in the range of 8–13 $\times$ 10^{-3} M; Papir *et al.*, 1998). These inhibitors can therefore serve as product analogues, as one of the products obtained in a normal enzymatic reaction is the cleaved amino-terminal amino acid of the substrate. Methionine was selected as the first candidate for the SGAP–analogue studies because of its relatively small size and relatively high affinity for SGAP (K_i = 8.7 mM).

The final model of the bound methionine inhibitor in the SGAP active site is shown in Fig. 5, where it is also compared with the corresponding region of the native enzyme.

In general, no significant conformational changes have been observed in the enzyme as a result of the inhibitor binding (except for the active site), as demonstrated by the low r.m.s. deviation (0.08 Å) between the structures of native SGAP and the SGAP–Met complex. The methionine inhibitor was found to be bound to the active-site zinc ions, displacing the zinc-bound water/hydroxide of the native enzyme in the solvent-accessible face of the active site (Fig. 5). The most significant contacts of the methionine inhibitor with SGAP are made by the free carboxylate group of the methionine which bridges the two zinc ions. These two Zn—O interactions are relatively short (and hence strong); however, they are not symmetrical (Zn—carboxylate distances of 2.23 and 1.98 Å for Zn1 and Zn2, respectively), supporting earlier suggestions that the two zinc ions are not equivalent in structure and/or binding. As demonstrated schematically in Fig. 6, the

methionine binding in the active site is further stabilized by a hydrogen bond between one of its carboxylate O atoms and the hydroxyl group of Tyr246 (2.95 Å) and a hydrogen bond between the other carboxylate O atom and the carboxylate group of Glu131 (2.76 Å). In addition, there are three hydrogen bonds between the methionine amine N atom (present probably as an $-NH_3^+$ group) and the carbonyl O atom of Arg202 (2.68 Å), a carboxylate O atom of Asp160 (2.76 Å) and the other carboxylate O atom of Glu131 (2.82 Å, Fig. 6).

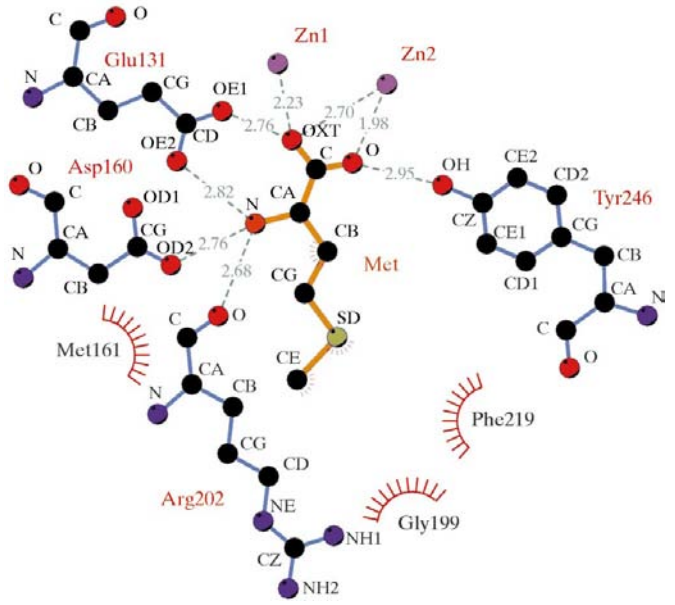

Figure 6
Interactions of the bound methionine with SGAP as demonstrated in a schematic diagram of the active-site region of the SGAP–Met complex. The protein bonds are shown in blue, the bound methionine (Met) bonds are shown in orange, the Zn atoms are shown in purple, while the rest of the atoms are in the standard atomic colors. Dashed lines indicate hydrogen bonds or ionic interactions, while 'radiating' spheres indicate hydrophobic contacts between the bound methionine (small spheres) and the neighbouring protein groups (larger spheres). [This figure was prepared with the program *Ligplot* (Wallace *et al.*, 1995).]

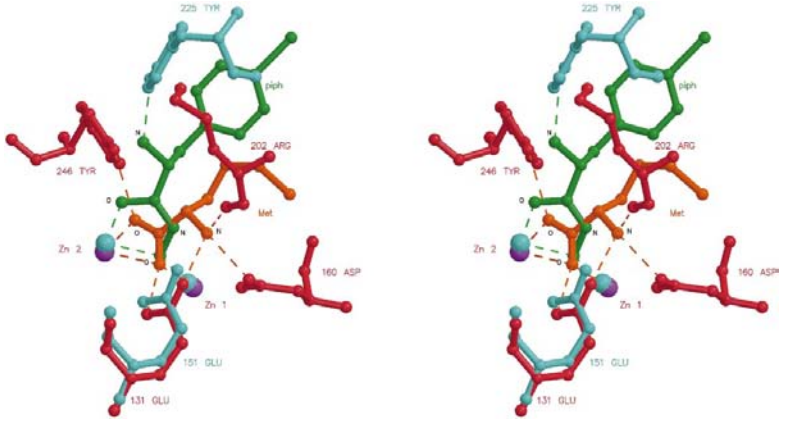

Figure 7
Stereoview comparison of the active site of the SGAP–Met complex (1.53 Å structure, red) with the active site of the AAP–PIPH complex (2.3 Å structure, cyan). Note the significantly different binding mode of PIPH (piph, green) relative to the binding mode of methionine (Met, orange) to the enzyme, especially the position and direction of the amino group (N) of the two inhibitors.

The side chain of the bound methionine inhibitor resides in a deep and distinct hydrophobic pocket, built mainly by Tyr246, Met161, Ala222, Phe219 and Tyr172. This deep hydrophobic pocket explains the preference of SGAP towards substrates with hydrophobic amino-terminus side chains that can map well into the pocket and interact with its aromatic residues. The methionine inhibitor interacts specifically with the enzyme-binding site through Met161, Gly201 and Phe219. No specific interactions with the enzyme are observed, however, for the methionine S atom, except for a potential indirect interaction *via* a disordered water molecule.

An interesting (and significant) change in the distance between the two co-catalytic Zn atoms is observed at the SGAP active site as a result of methionine binding (Fig. 5). In the SGAP–Met complex the Zn—Zn distance is 3.80 Å, while in the native enzyme the corresponding distance is only 3.60 Å (estimated error in these values is around 0.05 Å; Kleywegt & Brünger, 1996). Such elongation in the Zn—Zn distance has been previously reported for LAP upon binding of amastatin and bestatin (Burley *et al.*, 1990, 1991; Kim & Lipscomb, 1993) and for AAP upon binding of an hydroxamate inhibitor (Chevrier *et al.*, 1996); however, its relevance to substrate mode of binding or catalytic mechanism is not clear.

In addition to the important enzyme–inhibitor interactions discussed, the introduction of methionine into the active site of the enzyme significantly rigidified the floppy polypeptide loop consisting of the seven amino-acid residues Glu196–Arg202, as discussed above (see also Fig. 2). Especially effective in this regard is the hydrogen bond between the amine N atom of the methionine inhibitor and the carbonyl O atom of Arg202 of this loop (Fig. 6). The van der Waals interactions between Gly199 and Gly201 and the bound methionine side chain probably contribute to the conformational rigidity of this loop as well. The increased rigidity of the Glu196–Arg202 polypeptide loop in the SGAP–Met complex enabled for the first time the full identification of all of its amino-acid residues in the electron-density maps (Fig. 2). As a result, it is possible now to use the full three-dimensional structure of the SGAP active site for mechanism interpretations and structure-based design of inhibitors and analogues.

3.3. Comparison with corresponding structures of AAP

A comparison of the SGAP–Met structure with the complex of AAP with *p*-iodo-D-phenylalanine hydroxamate (PIPH; Chevrier *et al.*, 1996) shows a general resemblance in the double-zinc environment of the two systems (Fig. 7). In both structures, the inhibitor is bound as a bidentate ligand (with Zn—O bonds of 1.98 and 2.70 Å in SGAP and 2.12 and 2.35 Å in AAP) to one of the zinc ions (Zn2 in

SGAP), resulting in a pentacoordinated zinc, while bridging between the two zinc ions with only one of the oxygen ligands. In both structures, the two zinc ions move apart relative to the uncomplexed structure (0.20 Å in SGAP, 0.18 Å in AAP) and there is a significant interaction of a nearby glutamate (Glu131 in SGAP, Glu151 in AAP) with one of the zinc-bound O atoms of the analogue. The difference between the two structures originates mainly from the extra C atom in the PIPH hydroxamate ligand (compared with a carboxylate) and the different chirality of the two molecules (L for methionine; D for PIPH). These factors make the direction of binding and the position of the amino group of the PIPH hydroxamate inhibitor structurally different and probably less relevant compared with methionine and the 'normal' peptide substrates of these enzymes (Fig. 7).

Nevertheless, our results support the critical catalytic role suggested in AAP for the conserved active-site glutamate (Glu131 in SGAP, Glu151 in AAP). The bidentate binding of both inhibitors to the pentacoordinated zinc (Zn2 in SGAP) probably resembles the final stage of the catalytic reaction, when the free carboxylate of the cleaved N-terminus amino acid is stabilized by a tight interaction with the zinc cation and a hydrogen bond to the active-site conserved glutamate, similar to the stabilization of carboxylate inhibitor binding to CPA (Feinberg *et al.*, 1995; Greenblatt *et al.*, 1998). A more definitive assignment of a particular catalytic role to each of the zinc ions (*e.g.* substrate binding and activation for Zn1 and product binding and stabilization for Zn2) would require further structural studies of SGAP with various inhibitors and analogues. Such experiments are currently under way in order to clarify the catalytic mode of action of these double-zinc aminopeptidases.

3.4. Modelling of an enzyme–substrate complex

In order to obtain additional insight into the reaction mechanism of SGAP, a pseudo-substrate was docked manually into the active site by adding two alanine residues to the C-terminus of the bound Met inhibitor in such a way that they approximately follow the open channel that is observed on the surface of the protein. A water molecule and, in a parallel simulation, an hydroxide ion were added as potential nucleophiles in the position observed in the native SGAP structure. With a water molecule bound to the zinc ions, the substrate complex was not stable during the MD simulation and we were also unable to reproduce the geometry of the native uncomplexed structure. This led us to the conclusion that an hydroxide ion rather than a water molecule should be the nucleophile attacking the carbonyl C atom of the substrate.

The modelling study supported the relevance of the X-ray structure of the SGAP–Met complex, not only for the product situation but also to illustrate a substrate complex. Especially important in this respect is the confirmation of the interactions of the N-terminal amino-acid side chain and the deep hydrophobic pocket of the enzyme, as well as the position and interactions of the N-terminal amine group of the methionine (see Fig. 6). The modelling studies also suggested that the carbonyl O atom of the peptide bond to be hydrolyzed interacts with Zn2 and Tyr246 OH, which polarize the carbonyl group and would stabilize a potential oxyanion intermediate. The hydroxide ion is interacting with both zinc ions and forms a hydrogen bond to Glu131 $O^{\varepsilon 1}$. In a MD simulation, this led to an average distance between the hydroxide O atom and the carbonyl C atom in the substrate of 3.09 Å. The shortest distance observed for this interaction in the simulation was 2.76 Å, a distance which is short enough for a nucleophilic attack. However, the detailed mechanism of catalysis of SGAP, as well as related aminopeptidases, will require further experiments and calculations.

This work was supported in part by a grant from the German Federal Ministry of Education, Science, Research and Technology (BMBF) and the Israeli Ministry of Science (MOS) under the aegis of GBF – Gesellschaft für Biotechnologische Forschung GmbH, Braunschweig, and the Israel Academy of Sciences and Humanities – Israel Science Foundation.

References

Almog, O., Greenblatt, H. M., Spungin, A., Ben-Meir, D., Blumberg, S. & Shoham, G. (1993). *J. Mol. Biol.* **230**, 342–344.
Ben-Bassat, A., Bauer, K., Chang, S.-Y., Myambo, K., Boosman, A. & Chang, S. (1987). *J. Bacteriol.* **169**, 751–757.
Ben-Meir, D. & Blumberg, S. (1991). *Biologicals from Recombinant Microorganisms and Animal Cells: Production and Recovery*, edited by M. D. White, S. Reuveny & A. Shaffermann, pp. 55–61. Verlag Chemie.
Ben-Meir, D., Spungin, A., Ashkenazi, R. & Blumberg, S. (1993). *Eur. J. Biochem.* **212**, 107–112.
Brunger, A. T., Adams, P. D., Clore, G. M., Delano, W. L., Gros, P., Grosse-Kunstleve, R. W., Jiang, J. S., Kuszewski, J., Nilges, M., Pannu, N. S., Read, R. J., Rice, L. M., Simonson, T. & Warren, G. L. (1998). *Acta Cryst.* D**54**, 905–921.
Burley, S. K., David, P. R. & Lipscomb, W. N. (1991). *Proc. Natl Acad. Sci. USA*, **88**, 6916–6920.
Burley, S. K., David, P. R., Sweet, R. M., Taylor, A. & Lipscomb, W. N. (1992). *J. Mol. Biol.* **224**, 113–140.
Burley, S. K., David, P. R., Taylor, A. & Lipscomb, W. N. (1990). *Proc. Natl Acad. Sci. USA*, **87**, 6878–6882.
Chevrier, B., D'Orchymont, H., Schalk, C., Tarnus, C. & Moras, D. (1996). *Eur. J. Biochem.* **237**, 393–398.
Chevrier, B., Schalk, C., D'Orchymont, H., Rondeau, J.-M., Moras, D. & Tarnus, C. (1994). *Structure*, **2**, 283–291.
Cornell, W. D., Cieplak, P., Bayly, C. I., Gould, I. R., Merz, K. M., Ferguson, D. M., Spellmeyer, D. C., Fox, T., Caldwell, J. W. & Kollman, P. A. (1995). *J. Am. Chem. Soc.* **117**, 5179–5197.
Feinberg, H., Greenblatt, H. M., Behar, V., Gilon, C., Cohen, S., Bino, A. & Shoham, G. (1995). *Acta Cryst.* D**51**, 428–449.
Greenblatt, H. M., Almog, O., Maras, B., Spungin-Bialik, A., Barra, D., Blumberg, S. & Shoham, G. (1997). *J. Mol. Biol.* **265**, 620–636.
Greenblatt, H. M., Feinberg, H., Tucker, P. A. & Shoham, G. (1998). *Acta Cryst.* D**54**, 289–305.
Hoops, S. C., Anderson, K. W. & Merz, K. M. (1991). *J. Am. Chem. Soc.* **113**, 8262–8270.
Indig, F. E., Benayahu, D., Fried, A., Wientroub, S. & Blumberg, S. (1990). *Biochem. Biophys. Res. Commun.* **172**, 620–626.

Indig, F. E., Ben-Meir, D., Spungin, A. & Blumberg, S. (1989). *FEBS Lett.* **255**, 237–240.
Jones, T. A., Zou, J.-Y., Cowan, S. W. & Kjeldgaard, M. (1991). *Acta Cryst.* A**47** 110–119.
Kim, H. & Lipscomb, W. N. (1993). *Biochemistry*, **32**, 8465–8478.
Kleywegt, G. J. & Brünger, A. T. (1996). *Structure*, **4**, 897–904.
Lessel, U. & Schomburg, D. (1994). *Protein Eng.* **7**, 1175–1187.
Maras, B., Greenblatt, H. M., Shoham, G., Spungin-Bialik, A., Blumberg, S. & Barra, D. (1996). *Eur. J. Biochem.* **236**, 843–846.
Nagakawa, S., Yamada, T., Kato, K. & Nishimura, O. (1987). *Biotechnology*, **5**, 824–827.
Otwinowski, Z. (1991). *Proceedings of the CCP4 Study Weekend. Isomorphous Replacement and Anomalous Scattering*, edited by W. Wolf, P. R. Evans & A. G. W. Leslie, p. 80–86. Warrington: Daresbury Laboratory.
Papir, G., Spungin-Bialik, A., Ben-Meir, D., Fudim, E., Gilboa, R., Greenblatt, H. M., Shoham, G., Lessel, U., Schomburg, D., Ashkenazi, R. & Blumberg, S. (1998). *Eur. J. Biochem.* **258**, 313–319.
Pearlman, D. A., Case, D. A., Caldwell, J. W., Ross, W. S., Cheatham, T. E. III, Ferguson, D. M., Seibel, G. L., Singh, U. C., Weiner, P. K. & Kollman, P. A. (1995). *AMBER* 4.1. University of California, San Francisco, USA.
Roderick, S. L. & Matthews, B. W. (1993). *Biochemistry*, **32**, 3907–3912.
Schomburg, D. & Reichelt, J. (1988). *J. Mol. Graph.* **6**, 161–165.
Spungin, A. & Blumberg, S. (1989). *Eur. J. Biochem.* **183**, 471–477.
Strater, N. & Lipscomb, W. N. (1995). *Biochemistry*, **34**, 14792–14800.
Wallace, A. C., Laskowski, R. A. & Thornton, J. M. (1995). *Protein Eng.* **8**, 127–134.